Gigantic supramolecular assemblies built from dynamic hierarchical organization between inorganic nanospheres and porphyrins

Kirill Grzhegorzhevskii, Mohamed Haouas, Maxence Lion, Arthur Vashurin, Andrey Denikaev, Yuriy Marfin, Grigoriy Kim, Clément Falaise, Emmanuel Cadot

COMMUNICATION

Gigantic Supramolecular Assemblies built from Dynamic Hierarchical Organization between Inorganic Nanospheres and Porphyrins

Received 00th January 20xx,
Accepted 00th January 20xx

DOI: 10.1039/x0xx00000x

Kirill Grzhegorzhevskii,*[a] Mohamed Haouas,[b] Maxence Lion,[b] Arthur Vashurin,[c] Andrey Denikaev,[a] Yuriy Marfin,[c] Grigoriy Kim,[a, d] Clément Falaise,[b] and Emmanuel Cadot*[b]

Noncovalent ionic interactions between nanosized Keplerate-type capsules {Mo_{132}} and tetra-cationic porphyrins have been investigated in aqueous solution using small-angle X-ray scattering, ^{1}H NMR and photophysical methods. These complementary multiscale methods reveal the formation of large hybrid oligomers built from a short-range organization in which the cationic porphyrin is literally glued on the large POM surface. Whereas, local structuring appears strongly dependent on the dye:{Mo_{132}} ratio changing the morphology of the oligomers from linear to dense aggregates.

Porphyrin core represents a key part of many cofactors (e.g. vitamin B12) that are essential for living organisms.[1,2] This class of dyes exhibits striking catalytic and photophysical properties, making them highly appealing components to design multi-functional systems. In context, association of porphyrin derivatives with inorganic metal-oxo clusters such as polyoxometalates (POMs) has been used to develop catalytic and photovoltaic systems.[3–5] Although covalent attachment represents a popular strategy for designing such hybrid systems,[2,6] this approach has major drawbacks such as being time-consuming or the poor hydrolytic stability of covalent bonds. In contrast, the supramolecular approach could represent a straightforward synthetic route, offering both versatile and self-repairing systems, however the structures and the dynamics of such supramolecular aggregates remains largely poorly characterized or unknown.[7,8]

The Keplerate-type capsule $[Mo^{VI}_{72}Mo^{V}_{60}O_{372}(CH_3COO)_{30}(H_2O)_{72}]^{42-}$, notated hereafter {$Mo_{132}$}, is an anionic hollow sphere of 3 nm in diameter (see Fig. 1) exhibiting unique supramolecular behaviour in aqueous solution. For instance, this giant POM has been identified as able to *i*) recognize alkylammonium cations,[9] *ii*) to form large "blackberry" structures (20-1000 nm in size) *via* non-bonding interactions,[10–12] or iii) to encapsulate a wide variety of guest molecules.[13–16] Recently, it was observed that {Mo_{132}} is able to act as efficient catalyst for hydrogen evolution when associated with porphyrin derivatives as photosensitizers.[17] However, no structural information at molecular or macromolecular level is available for such hybrid assembly that remains essential to better understand reactions mechanism of the photocatalytic tandem. Herein, we report multiscale investigations of supramolecular interaction between the giant polyanion {Mo_{132}} and the tetra-cationic porphyrin 5,10,15,20-tetrakis(4-methylpyridyl)porphyrin (see Fig. 1), denoted H_2TMPyP, introduced as tosylate salt (TOS).

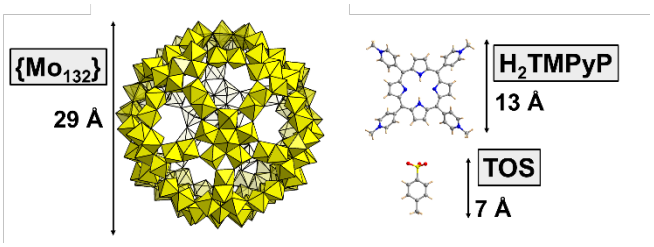

Fig. 1: Structural representations of the molecular components involved in the formation of gigantic supramolecular assemblies. The Keplerate-type POM $[Mo_{132}O_{372}(CH_3COO)_{30}(H_2O)_{72}]^{42-}$ (or {Mo_{132}}) is a nanosized inorganic hollow sphere. The tetra-cationic porphyrin $C_{44}H_{38}N_8^{4+}$ (or H_2TMPyP) is a planar dye that comprises a porphyrin core and four N-methylpyridinium side groups. This cationic dye was associated to tosylate anion $C_7H_7O_3S^-$ (or TOS) as counterion.

At first, small-angle X-ray scattering (SAXS) have been used to characterize the 0.1 mM aqueous solutions of {Mo_{132}} containing different amounts of porphyrin (from 0.5 to 40 eq.). It is worth to mention that SAXS technique has been already used successfully for studying large POMs in solution.[18–20] In absence of dye, the SAXS curve exhibits three well-defined oscillations (Fig. 2) similar to that calculated for discrete {Mo_{132}} (Fig. S1). The *R*g value determined by using Guinier law

[a] *Ural Federal University, Institute of Natural Sciences and Mathematics, 19 Mira St., Ekaterinburg, Russia.*
[b] *Institut Lavoisier de Versailles CNRS, UVSQ, Université Paris-Saclay, Versailles, France.*
[c] *Ivanovo State University of Chemistry and Technology, Sheremetevsky str., 7, 153000 Ivanovo, Russia.*
[d] *Institute of Organic Synthesis Ural Branch of the Russian Academy of Sciences 22 AkademicheskayaSt.,620990 Ekaterinburg, Russia.*
† Electronic Supplementary Information (ESI) available: [details of any supplementary information available should be included here]. See DOI: 10.1039/x0xx00000x

supported by the PDDF analysis is fully consistent with the expected values for dispersed Keplerate-type anions in aqueous solution (see Fig. S2-S3). In the presence of increasing amount of H_2TMPyP, no or very weak modifications are observed at high *q* value (> 0.1 Å^{-1}) demonstrating that Keplerate ions remain intact in such conditions. However, abrupt increase of the scattering intensity is observed at low *q* consistent with the presence of large aggregates whose fractal dimension can be anticipated from the negative slope of the scattering intensity (Fig. 2A). The SAXS curves obtained for 0.5 and 1 eq. of H_2TMPyP exhibit negative slope of -0.9 and -1.2, respectively, consistent with the presence of quasi-linear aggregates built from the electrostatically-induced oligomerization involving POMs and the planar organic tetra-cations. Increasing further the dye content leads to a structural reorganization evidenced by the stronger power law dependence observed for POM: H_2TMPyP ratio larger than 2 eq. (slope = -1.7). Such a structural change could result from the formation of branched or cross-linked polymeric hybrid aggregates. For ratio larger than 5, the scattering curve shows two linear regimes (Fig. 2B) highlighted by slopes of −1.6 and -3.1 for the *q* ranges 0.01-0.04 and 0.05-0.15 Å^{-1}, respectively. This shape suggests that the dye-{Mo_{132}} aqueous mixture contains branched polymeric aggregates built from dense Keplerate-based assemblies with a diameter varying from 7 to 12 nm (Fig. S5). For high contents in porphyrin *e.g.* 40 eq , the SAXS curves exhibit similar signature than those observed for 5 eq., except for the first oscillation significantly which becomes broader and significantly shifted from 0.25 to 0.22 Å^{-1}. Such a SAXS profile shows that the long-range organization of the hybrid aggregates is fully maintained while short-range structural modifications occur at the close vicinity of the Keplerate. To provide information about the interactions occurring at the molecular level between H_2TMPyP and {Mo_{132}}, ^{1}H NMR titration of 0.25 mM porphyrin D_2O solution has been first performed. Increasing the POM content from POM:dye ratio 1:100 up to 1:20 resulted in progressive decrease in ^{1}H NMR signals intensity of aromatic protons (9.3-8.8 ppm) of porphyrin (Fig. S7). Although quite unaffected for ratios less than 1:40, their linewidth becomes suddenly very broad at 1:20 ratio for finally disappearing at 1:10 and larger ratio (Fig. 3). Interestingly, the signals of benzene core in TOS anion (7.06 and 7.46 ppm) behave differently, showing a significant gradual broadening until a POM:H_2TMPyP ratio of 1:20. However, the TOS signals recover intensity and narrow again as doublet for ratios larger than 1:10. At the same time, these protons undergone a significant deshielding (7.30 and 7.62 ppm). This means that TOS anions are involved in fast chemical exchange regime within the large hybrid aggregates and this process is progressively slowing down with the formation of the supramolecular assembly until POM:H_2TMPyP = 1:20. For larger POM content, the TOS anions remain mostly isolated as solvated ions as shown by the reversed NMR titration of 0.1875 mM {Mo_{132}} solution for which the signals of TOS preserve fine structure. (Fig. 3). We also found that the NMR signal of acetate ligands inside the Keplerate cavity at 0.77 ppm disappears gradually when the

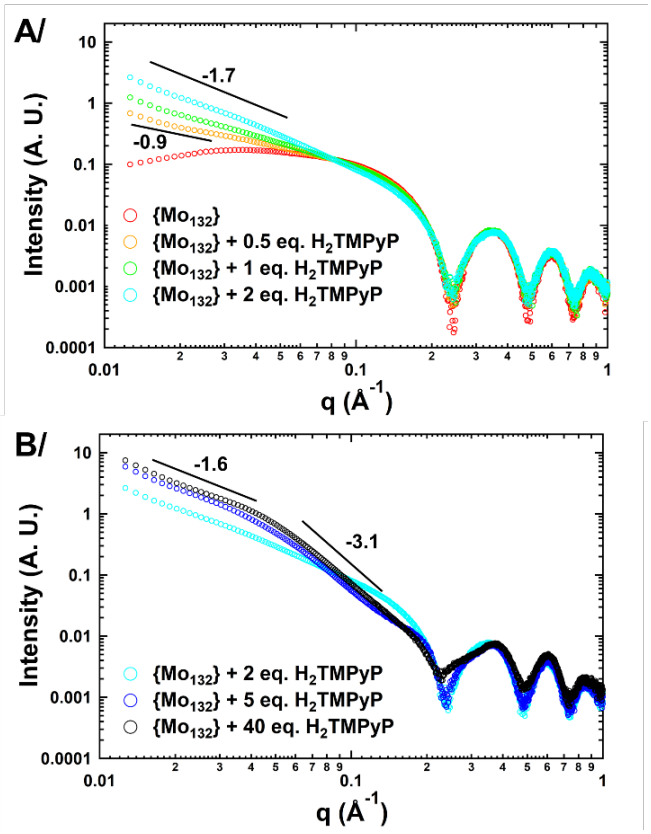

Fig. 2: The log(*q*)-log(I(*q*)) scattering curves of aqueous solutions containing 0.1 mM {Mo_{132}} and various amounts of H_2TMPyP (A: from 0 to 2 eq.; B: from 2 to 40 eq.).

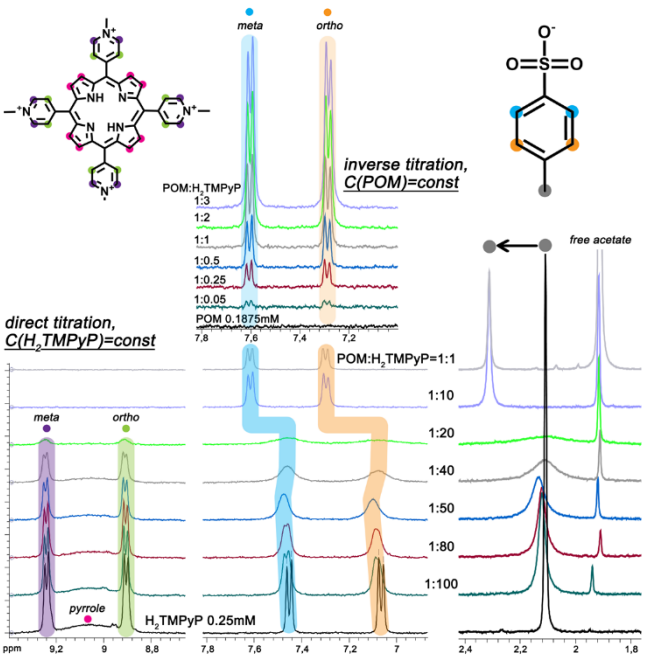

Fig. 3: ^{1}H NMR spectra (in D_2O) for different molar ratio POM:porphyrin at constant H_2TMPyP concentration of 0.25 mM (direct titration) and at constant {Mo_{132}} concentration of 0.1875 mM (inverse titration).

ratio POM:dye increases (Fig. S6), due to the very low diffusion coefficient of the Keplerate ions embedded within large supramolecular structures. Analysis of these results leads to the following statements: i) H_2TMPyP species interacting with Keplerate anions are NMR silent, whereas ii) TOS anions also are involved in the large supramolecular hybrid aggregates as ion-pairing arrangements with H_2TMPyP in the molar ratio range 1:100-1:20. In contrast, with increasing of POM content (for larger ratio than 10), TOS anions are not involved in supramolecular structures which are built exclusively from ionic interaction between POM and H_2TMPyP. In such a scenario, the TOS anions were released as isolated and solvated species. In line with the 42- ionic charge of $\{Mo_{132}\}$ and the four positive charges of H_2TMPyP cation, the 1:10 ratio corresponds nearly to the stoichiometry of the electric balance. Then, the number of porphyrin interacting per Keplerate ions have been also determined by integrating the NMR data into a Langmuir model (Fig. S7), which is consistent with a maximal capacity of about 18-19 dyes per POM. This high number suggests the formation of a double porphyrin shell around the POM capsule where the first layer involves direct contacts between POM and dyes and the second shell should consist of porphyrins interacting with first layer through intercalated TOS anions through π- π stacking. Furthermore, the self-assembly process between the $\{Mo_{132}\}$ and H_2TMPyP has been investigated also by photophysical methods, namely UV-vis spectroscopy, steady-state photoluminescence (PL) and photoluminescence excitation (PLE). Such techniques require diluted systems due to the high molar absorptivity of the components. UV-Vis spectra (Fig. S8-S9) showed only a weak red shift of B band (Soret) and Q-bands of porphyrin in presence of POM. Besides, the fluorescence properties of pure H_2TMPyP are related to the monomer and the excimer emission or to equilibrium between free base form and partially deprotonated one.[21] Within the 5-500 μM range, the PL spectra remain nearly unchanged (Fig. S10). However, the Soret band diminishes in PLE spectra (Fig. S11) as a consequence of FRET and/or π-stacking with TOS anions[22] accompanied with PICT[23]. For molar ratio POM:porphyrin = 1:1, the PL quenching is incomparably stronger than in pure porphyrin solution showing a 320-fold decreased PL intensity at 711 nm. Such an effect is consistent with a charge transfer (CT) process according to the HOMO/LUMO positions at -5.9/-4.16 and -5.8/-4.19 eV for porphyrin[24] and Keplerate[25], respectively. Interestingly, CT-process was also observed[26] in another macrocyclic oligopyrrole dye covalently bound to POM $\{P_2V_3W_{15}O_{62}\}^{9-}$.

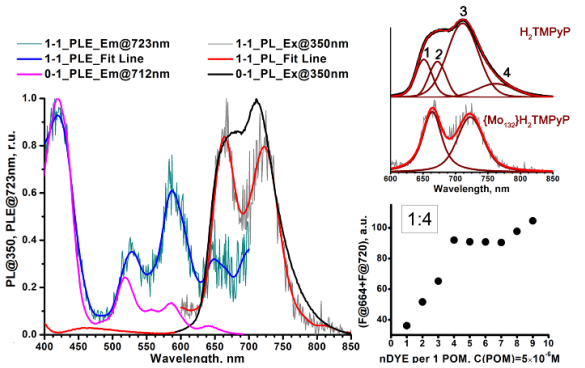

Fig. 4: Normalized PL (excited at 350 nm), PLE (emission at 712-723 nm) spectra of pure porphyrin aqueous solution at 5 μM (0-1 sample) and associate $\{Mo_{132}\}(H_2TMPyP)_n$ at C(porphyrin) = 5 μM and 1:1 molar ratio (1-1 sample). *Inserts*: *black spots* - sum of fluorescence peaks intensity of H_2TMPyP at 664 and 720 nm plotted against dye:POM molar ratio; *red lines* - deconvolution (with Voight function) of PL spectra (excited at 350 nm) of pure H_2TMPyP and the supramolecular hybrid aggregate at 1:1 molar ratio.

Generally, PL spectrum loses the second and fourth components (Fig. 4, insert) and band at 711 nm shifts to 723 nm. In PLE spectrum the contribution of Q_{1x} band near 585 nm increases significantly (even after correction on POM absorption). As only free porphyrins contribute to PL and PLE spectra, such a behavior can be simply attributed to concentration effect. Besides, the intensity sum of the emission bands at 664 and near 722 nm plotted against POM:dye ratio is consistent with an average stoichiometry of four porphyrins per one Keplerate (Fig. 4**,** insert). Then, the four positive charges localized at the periphery of the porphyrin (accessible on both sides of molecular plane), could be shared by two adjacent POMs like as a ditopic linker able to associate two building blocks. At last, thermodynamic parameters featuring the $\{Mo_{132}\}$-H_2TMPyP interactions have been determined from Stern-Volmer titration, using the full equation for 1:1 molar ratio after correction on the inner filter effect[27] (see ESI†). The Stern-Volmer plot does not lead to linear function (Fig. S13) pointing out to complex intermolecular interactions for this system. The static quenching mechanism in $\{Mo_{132}\}$-H_2TMPyP pair is confirmed (see Fig. S14) since lifetimes of excited state are preserved: 5.4 ± 0.2 and 5.1 ± 0.2 ns for H_2TMPyP and aggregate obtained with one H_2TMPyP per $\{Mo_{132}\}$, respectively. Besides, binding constant (K_{SV} = 21·10^9) and related free Gibbs energy $\Delta_r G^*_{298}$ = -RTlnK_{SV} ($\Delta_r G^*_{298}$ = -58.8 kJ·mol^{-1}) are consistent with very strong attractive interactions between the Keplerate and porphyrin ionic species. These solution studies have revealed that strong coulombic interactions between H_2TMPyP and $\{Mo_{132}\}$ probably supported

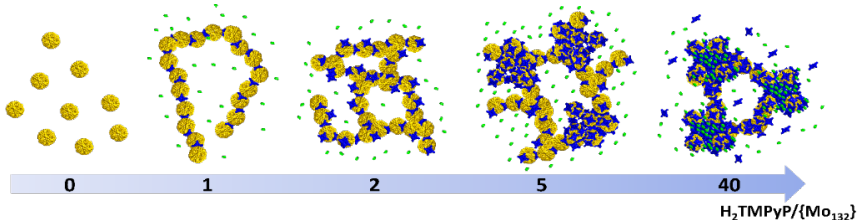

Fig. 5. Schematic representation of hybrid supramolecular aggregates built from Keplerate (yellow), H_2TMPyP (blue) and TOS (green). As the H_2TMPyP:POM ratio (noted *R*) increases, the POM-porphyrin system gives rise to quasi-linear oligomers (*R* = 1), which then self-arrange into branched-type oligomers (*R* = 2). For 5 < *R* < 10, the hybrid assembly becomes denser giving rise to close-packed aggregates, while for *R* > 10, these packed aggregates intercalates tosylate anions strongly immobilized within a porphyrin-based multi-shell around the inorganic capsules.

by solvent effects that relies the hydrophobic nature of the ionic species gives rise to the formation of gigantic supramolecular oligomers in which both short- and long-range organizations are controlled by the H_2TMPyP:{Mo_{132}} ratio (Fig. 5). In short, for low H_2TMPyP content (1-2 eq per POM), porphyrins behave as ditopic linker producing either rod-like supramolecular oligomers or branched aggregates. For H_2TMPyP a content larger than 5 eq., dense supramolecular hybrid arises from self-rearrangements into closely packed {Mo_{132}}-porphyrin species within the oligomers. For high porphyrin concentrations (> 10 eq.), the long-range structural organization remains mostly unchanged while important modifications of the molecular interactions between primary building blocks are depicted. In such conditions, the Keplerate surface should be decorated by about 18-19 dyes that intercalate TOS anions as guests into a double shell structure.

Aging the {Mo_{132}}-H_2TMPyP mixtures leads to flocculation whose rates vary from minutes to weeks depending on the concentration and on the POM:dye ratio. Typically, the flocculation process is faster for the POM:dye ratio close to 10, corresponding roughly to the electric balance. Infrared and Raman analysis showed that dry flocs are mostly composed of Keplerate and dye (Fig. S15-S17). Interestingly, Raman spectra revealed that the normal vibration modes of porphyrin shift to higher energy on 5-12 or 1-3 cm^{-1} level (except for δ(*pyr*): 1642→1639 cm^{-1} (A_{1g})). Such a trend is consistent with an increase of the rigidity of porphyrin, probably due to planar interactions with rigid POM.

In summary, very strong associations between Keplerate-type capsule and H_2TMPyP give rise to efficient charge transfer while structure of the resulting supramolecular oligomers can be monitored via composition of the three-component system POM/porphyrin/tosylate. This is the way for smart-design of novel hybrid materials based on porphyrins.

This work was supported by Russian Science Foundation: Project No.21-73-00311 in the part of synthesis and samples characterization and a public grant overseen by the French National Research Agency as part of the "Investissements d'Avenir" program (Labex Charm3at, ANR-11-LABX-0039-grant). We acknowledge SOLEIL and Dr. J. Perez for synchrotron facilities and assistance in using beamline SWING.

Notes and references

1 K. Sugiyasu, S. Ogi and M. Takeuchi, *Polymer Journal*, 2014, **46**, 674–681.
2 R. Lamare, R. Ruppert, C. Boudon, L. Ruhlmann and J. Weiss, Chemistry – A European Journal, 2021, 27, 16071–16081.
3 C. Zou, Z. Zhang, X. Xu, Q. Gong, J. Li and C. Wu, J. Am. Chem. Soc., 2012, 134, 87–90.
4 Z. Huo, A. Bonnefont, Y. Liang, R. Farha, M. Goldmann, E. Saint-Aman, H. Xu, C. Bucher and L. Ruhlmann, Electrochimica Acta, 2018, 274, 177–191.
5 G. Paille, M. Gomez-Mingot, C. Roch-Marchal, B. Lassalle-Kaiser, P. Mialane, M. Fontecave, C. Mellot-Draznieks and A. Dolbecq, J. Am. Chem. Soc., 2018, 140, 3613–3618.
6 Y. Zhu, Y. Huang, Q. Li, D. Zang, J. Gu, Y. Tang and Y. Wei, Inorg. Chem., 2020, 59, 2575–2583.
7 A. Tsuda, E. Hirahara, Y. S. Kim, H. Tanaka, T. Kawai and T. Aida, Angew. Chem. Int. Ed., 2004, 43, 6327–6331.
8 A. Yokoyama, T. Kojima and S. Fukuzumi, Dalton Trans., 2011, 40, 6445–6450.
9 N. Watfa, D. Melgar, M. Haouas, F. Taulelle, A. Hijazi, D. Naoufal, J. B. Avalos, S. Floquet, C. Bo and E. Cadot, J. Am. Chem. Soc., 2015, 137, 5845–5851.
10 P. P. Mishra, J. Pigga and T. Liu, J. Am. Chem. Soc., 2008, 130, 1548–1549.
11 J. Zhang, D. Li, G. Liu, K. J. Glover and T. Liu, J. Am. Chem. Soc., 2009, 131, 15152–15159.
12 F. Haso, D. Li, S. Garai, J. M. Pigga and T. Liu, Chemistry – A European Journal, 2015, 21, 13234–13239.
13 A. Ziv, A. Grego, S. Kopilevich, L. Zeiri, P. Miro, C. Bo, A. Müller and I. A. Weinstock, J. Am. Chem. Soc., 2009, 131, 6380–6382.
14 R. Carr, I. A. Weinstock, A. Sivaprasadarao, A. Müller and A. Aksimentiev, Nano Lett., 2008, 8, 3916–3921.
15 R. W. Pow, W. Xuan, D.-L. Long, N. L. Bell and L. Cronin, Chemical Science, 2020, 11, 2388–2393.
16 S. Chakraborty, A. Shnaiderman Grego, S. Garai, M. Baranov, A. Müller and I. A. Weinstock, J. Am. Chem. Soc., 2019, 141, 9170–9174.
17 A. Panagiotopoulos, A. M. Douvas, P. Argitis and A. G. Coutsolelos, ChemSusChem, 2016, 9, 3213–3219.
18 D. Sures, M. Segado, C. Bo and M. Nyman, J. Am. Chem. Soc., 2018, 140, 10803–10813.
19 C. Falaise, S. Khlifi, P. Bauduin, P. Schmid, W. Shepard, A. A. Ivanov, M. N. Sokolov, M. A. Shestopalov, P. A. Abramov, S. Cordier, J. Marrot, M. Haouas and E. Cadot, Angew. Chem. Int. Ed., 2021, 60, 14146–14153.
20 O. Renier, C. Falaise, H. Neal, K. Kozma and M. Nyman, Angew. Chem. Int. Ed., 2016, 128, 13678–13682.
21 K. Kalyanasundaram, Inorg. Chem., 1984, 23, 2453–2459.
22 M. Makarska-Bialokoz, J. Mol. Struct., 2015, 1081, 224–232.
23 C. A. Guido, B. Mennucci, D. Jacquemin and C. Adamo, Physical Chemistry Chemical Physics, 2010, 12, 8016.
24 K. Kalyanasundaram and M. Neumann-Spallart, J. Phys.Chem., 1982, 86, 5163–5169.
25 V. Fazylova, N. Shevtsev, S. Mikhailov, G. Kim, A. Ostroushko and K. Grzhegorzhevskii, Chem. Eur. J., 2020, 26, 5685–5693.
26 R. Pütt, P. Kozłowski, I. Werner, J. Griebel, S. Schmitz, J. Warneke and K. Y. Monakhov, Inorg. Chem., 2021, 60(1), 80-86.
27 M. van de Weert and L. Stella, *J. Mol. Struct.*, 2011, **998**, 144-150.